fact assures that the obtained alignment is not compromised by an error of τ in the range of milliseconds.

VII. CONCLUSIONS

The electroluminescence in some alkali iodide crystals has been interpreted according to an impact-ionization model. The dependence of the photoemission on the temperature and on the electric field is explained, with the mentioned mechanism, under the following assumptions:

(a) Potential barriers are formed at the metal-insulator interface. The maximum field in the barrier is proportional to the applied voltage (Rose-type barrier).

(b) Fowler-Nordheim tunnel injection is responsible for the electron emission from the negatively biased electrode.

Moreover, the brightness waves of the electroluminescence at different temperatures suggest that (i) hole injection from the metal into the crystals is negligible or nonexistant; (ii) trapped electrons can be freed by means of field-assisted thermal ionization.

The obtained results show the possibility of studying the injection and transport processes in low-conductivity insulating crystals by observing the photoemission under high electric fields.

*Work supported by the Gruppo Nazionale Struttura della Malerie of the Comitato Nazionale delle Ricerche..

[1](a) A. N. Georgobiani and N. P. Golubeva, Opt. Spektrosk. 12, 802 (1962) [Opt. Spectrosc. 12, 455 (1962)]; (b) S. Unger and K. Teegarden, Phys. Rev. Lett. 19, 1229 (1967); (c) H. Windischmann, Ph.D. thesis (The University of Rochester, 1970) (unpublished); (d) R. Onaka, H. Okuni, and K. Oomae, in International Conference on Luminescence, Leningrad, 1972 (unpublished).

[2]C. Paracchini, Phys. Rev. B 4, 2342 (1971).

[3]C. Paracchini, in Ref. 1(d).

[4]C. Paracchini, Phys. Rev. B 7, 1603 (1973).

[5]See, for example, N. Klein, in *Advances in Electronics Electron Physics*, edited by L. Marton (Academic, New York, 1969), Vol. 26, pp. 309–424.

[6]W. Ch. Van Geel, A. C. Pistorius, and B. C. Bouma, Philips Res. Rep. 12, 6 (1957).

[7]R. Cooper and C. T. Elliott, Br. J. Appl. Phys. 17, 481 (1966); J. Phys. D 1, 121 (1968).

[8]H. Baessler, G. Vanbel, K. Rasskopf, and K. Reinke, Z. Naturforsch. A 26, 814 (1971).

[9]S. T. Hsu, Appl. Phys. Lett. 20, 20 (1972).

[10]D. Pooley and W. A. Runciman, J. Phys. C 3, 1815 (1970).

[11]The formation of space-charge layers near the junction with a metal is commonly assumed in semiconductors, but it is a still discussed problem in wide-gap and high-resistivity insulators (Ref. 12); the study of electroluminescence should be a useful way to investigate this problem.

[12]See, for example, J. G. Simmons, *DC Conduction in Thin Films* (Mills and Boon, London, 1971); J. G. Simmons, J. Phys. Chem. Solids 32, 1987 (1971).

[13]J. J. O'Dwyer, J. Phys. Chem. Solids 28, 1137 (1967).

[14]A. Rose, Helv. Phys. Acta 29, 199 (1956).

PHYSICAL REVIEW B VOLUME 8, NUMBER 2 15 JULY 1973

Magneto-optical Study of a Charge-Transfer Band in Vanadium-Doped MgO†

F. A. Modine

Solid State Division, Oak Ridge National Laboratory, Oak Ridge, Tennessee 37830

(Received 18 September 1972)

A study of the magnetic circular dichroism and optical absorption associated with a band at 5.15 eV in vanadium-doped MgO is presented. The band is assigned to an electron transition from an orbital predominantly on the oxygen ligands of the V^{3+} ion to an orbital predominantly on the V^{3+} ion. Theory for the magnetic circular dichroism originating from the orbitally degenerate ground state is proposed, and the result of an analysis is found to be consistent with the presence of a dynamical Jahn-Teller effect in the ground state. A classification of the excited-state symmetry is made which implies a reversal from the conventional ordering of the πt_{1u} and πt_{2u} ligand-orbital energy levels.

I. INTRODUCTION

The magnetic circular dichroism (MCD) of a charge-transfer band associated with the V^{3+} ion in MgO is of interest for several reasons. The non-Kramers ground state of the V^{3+} ion is expected to be Jahn-Teller active in cubic MgO and there may be a modification of the ground-state magnetic properties by the electron-lattice interaction. However, these magnetic properties are not easily studied. The ion is undetected in MgO by electron paramagnetic resonance even though the less stable V^{2+} ion is commonly seen. The magnetic circular dichroism is, nevertheless, applicable to an investigation of the magnetic properties.

The optical aspects of the study are also of interest and the study of a charge-transfer band is

interesting for its own sake. These intense absorption bands, which originate in electron transitions between an impurity and its ligands, are still poorly understood. Ligand-orbital theory predicts many more bands than are ordinarily observable and there is consequently a shortage of experimental evidence to compare with theory. Magnetic circular dichroism is useful because it gives excited-state information which can reveal the symmetry of the charge-transfer states.

The application of the MCD to the V^{3+} ion in MgO is additionally of some theoretical interest. Although the theory of MCD originating in optical transitions from orbitally nondegenerate ground states is now well established, this theory does not extend to the orbitally degenerate V^{3+} ground state.

The ground state of the V^{3+} ion in MgO has been studied by Brabin-Smith and Rampton[1] using acoustical paramagnetic resonance (APR) and by Modine[2] using MCD. In both studies, a zero-field splitting of approximately 10 cm^{-1} and a small-g value were deduced. (Brabin-Smith and Rampton give $g = 0.69$ for an effective spin of one.) In both cases, a tetragonal site symmetry was proposed and evidence for a dynamical Jahn-Teller effect was recognized. Furthermore, as a result of both studies an energy-level diagram was proposed that placed a doublet level above a lowest singlet level. However, the level symmetry assignments were different.

Theoretical analyses of the Brabin-Smith–Rampton APR results have been made by Bates *et al.*[3] and Ray,[4,5] and two still-different ground-state energy-level diagrams were proposed. However, the model proposed by Ray appears to be the most satisfactory. Ray places a triplet level above a lowest nonmagnetic doublet and avoids the introduction of a tetragonal site symmetry by explaining the zero-field splitting in terms of a Jahn-Teller effect. Furthermore, Ray's analysis gives a better agreement with the APR results.

More recently, the APR spectrum of vanadium-doped MgO has been measured and subjected to further analysis by Buisson and Nahmani.[6,7] These investigators propose an energy-level diagram which is essentially in agreement with that of Ray, but they give a somewhat different explanation of the APR spectra and the ground-state splittings. From their measurements, they deduce a g value of 0.67 and a zero-field splitting of 7 cm^{-1}.

In the present work, the optical absorption and MCD measurements are presented and analyzed in terms of the ground-state model proposed by Ray.

II. EXPERIMENTAL METHODS

The vanadium-doped MgO crystals used in the study had been grown from a melt. The vanadium content was roughly estimated as a few tenths of a percent. Paramagnetic resonance studies showed that Mn^{2+}, Cr^{3+}, and Fe^{3+} were also present as impurities. The original crystals could be cleaved into thin plates of optical quality and were suitable for optical-absorption measurements, but they were still too dense for MCD measurements. The crystal which was used for most of the MCD measurements was therefore further prepared by grinding and polishing with corundum and diamond powders and had the dimensions of $4 \times 3 \times 0.1$ mm. The optical quality of the polished crystal was not as good as that of cleaved crystals, but was for the most part restored by heat treatment. After treatment at 1000 °C in an argon atmosphere, the crystal was rapidly cooled (quenched) to room temperature in order to reduce association of the V^{3+} ion with charge-compensating vacancies.

The light source used for the MCD measurements was a high-pressure xenon arc lamp. The light was focused onto a quartz-prism double monochromator, and the beam emerging from the monochromator was polarization modulated at 50 kHz with a modulator of the stress birefringent type.[8] This beam was focused onto the sample which was mounted either in a cold-finger Dewar placed between the poles of an electromagnet, or in the bore of a superconducting solenoid in an immersion Dewar. The electromagnet has an axial bore, giving optical access along the direction of the magnetic field. Light passing through the sample was focused onto a photomultiplier tube. The phototube signal, which is proportional to the MCD, was amplified and measured with a synchronous detector. The magnitude of the signal was calibrated against the circular dichroism of a 1-mg/ml water solution of d-10 camphorsulfonic acid. The circular dichroism of 1 cm of this solution was taken as $+0.0215$ at 290 nm.[9]

High-temperature MCD measurements were made using the electromagnet and cold-finger Dewar. Most of the measurements were taken using the superconducting solenoid and an immersion Dewar with the sample in liquid helium. Measurements were taken below 4.2 K, while pumping on the liquid helium, and were extended to above 4.2 K by pumping the Dewar dry and allowing the solenoid to warm up. The niobium solenoid could be operated up to 9 K at low magnetic fields. A thermocouple mounted in the solenoid bore was used to monitor sample temperature.

Optical-absorption measurements were made with a Cary model No. 15 or a Cary model No. 14 spectrophotometer. The effect of oxidation and reduction on the absorption spectrum was examined and these experiments utilized a Centorr 2500 °C controlled-atmosphere furnace.

III. EXPERIMENTAL RESULTS

An optical-absorption spectrum of a vanadium-doped MgO crystal is shown in Fig. 1. The two bands in the visible are assignable to transitions within the Stark-split d shell of the V^{3+} ion and are similar to bands in a visible spectrum reported by Sturge.[10] However, a noticeable difference is that the band near 3 eV appears at slightly higher energy than in Sturge's spectrum. A possible explanation[2] is that the absorption energy is perturbed by charge-compensating vacancies. Only the much more intense band in the near uv will be considered in detail here. The classification of this band as originating with an allowed ligand to V^{3+} electron transfer is based upon the optical-absorption spectrum and is confirmed by a detailed analysis of the MCD spectrum.

Figure 2 shows the change induced in the uv absorption by oxidation and reduction. Heat treatment in hydrogen changes the valence of the vanadium and decreases the band absorbance by about a factor of 2. This is consistent with the result of a similar study of the visible spectrum by Sturge[10] and supports the identification of the band as due to vanadium in a trivalent form. A further heat treatment in oxygen restores the band and adds absorption in the wings of the band. This increase in the wings is presumably due to trivalent iron which is normally in a divalent form.[11] Rapid cooling after heat treatment in argon causes the band to narrow. This possibly results from a decreased association of the V^{3+} with charge compensators.

A classification of the transition as allowed is based upon the high intensity of absorption. The classification of the band as owing to a ligand to V^{3+} electron transfer is based upon the transition energy. Such transitions appear typically in the near uv.[12] There is also a recognized tendency for the energy of such bands to decrease with

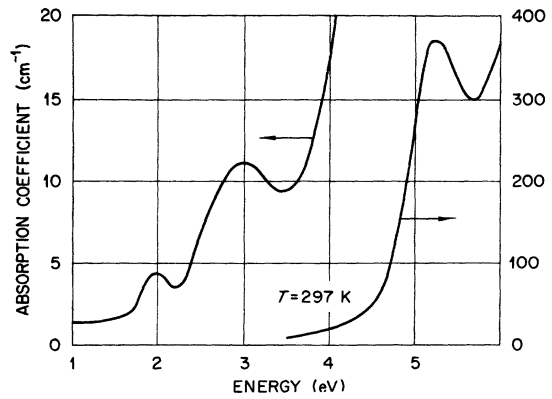

FIG. 1. Optical-absorption spectrum of a vanadium-doped MgO crystal.

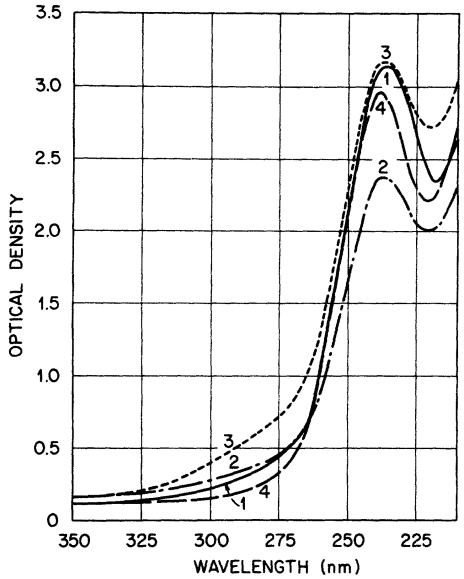

FIG. 2. Changes induced in the optical-absorption spectrum by consecutive treatment: (1) an untreated crystal shows only negligible change after 2 h at 1400 °C in argon; (2) after 4 h at 1400 °C in hydrogen; (3) after 2 h at 1400 °C in oxygen; (4) after 2 h at 1000 °C in argon and rapid cooling.

oxidizing character of the metal ion or reducing character of the ligands.[12,13] The placement of the V^{3+} band at somewhat higher energy than the known 4.3-eV Fe^{3+} band[11] appears to be consistent with this trend.

A representative MCD spectrum is shown with the optical absorption in Fig. 3. At low temperatures and high magnetic fields, continuous and virtually noise-free MCD spectra were recorded. The MCD spectrum is absorptionlike and no absorption-derivative-like character was discernable even at room temperature. Zeeman splittings which can give a derivativelike character are therefore absent or unresolved.

The MCD is very temperature dependent. In fact, the sign of the MCD changes from positive to negative between room and liquid-nitrogen temperature. The temperature dependence of the peak MCD, which is at 5.15 eV, is shown in Fig. 4. The change in the MCD varies reasonably as the inverse temperature, but the MCD saturates near liquid-helium temperature. With the exception of the few high-temperature points, the data were taken at low magnetic field to ensure that they are linear with field. The low magnetic field, bubbling of the liquid helium, and uncertainty in sample temperature contribute to the scatter of the data.

IV. THEORY

The experimental data consist of the polarization-independent optical-absorption spectrum and

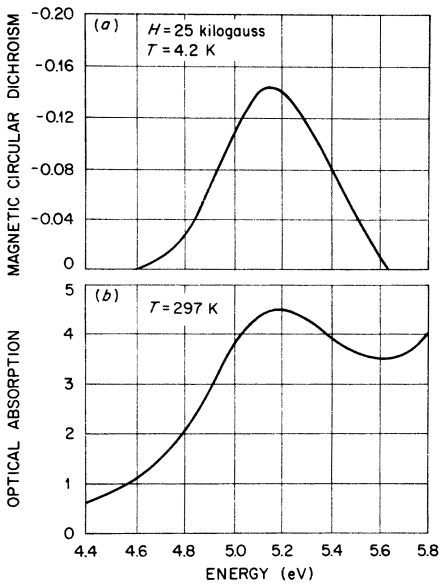

FIG. 3. (a) MCD $= t\Delta\alpha$, where t is sample thickness and $\Delta\alpha$ is the difference between the optical-absorption coefficient for left- and right-circular polarization. (b) Optical absorption $t\alpha$ is the ln of the ratio of incident to transmitted light intensity.

the MCD spectrum, which is a function of magnetic field and temperature. The optical absorption is defined by the base e absorbance ($t\alpha$, where t is crystal thickness and α is the absorption coefficient). The MCD ($t\Delta\alpha$) is defined as the difference in absorption of left- and right-circularly polarized light. The theoretical problem is, of course, to find a means of interpreting and obtaining information from these spectra.

The quantum theory of optical-absorption spectra is well known.[14,15] Extensions of this theory to MCD have been given in several recent papers.[16–19] As a result, the theory of MCD originating with optical transitions from orbitally nondegenerate ground states is now reasonably well established. For such cases, it has been shown that a moment analysis of the MCD spectrum will give excited-state parameters, such as magnetic moments and spin-orbit splittings, that are unmodified by the presence of a Jahn-Teller effect. Even so, the analysis will reveal a Jahn-Teller effect if it is present.

However, the analysis and interpretation of an MCD spectrum are much less certain in the case of an orbitally degenerate ground state which is Jahn-Teller active. Orbital degeneracy in the excited state is treatable because the electron wave functions can be extricated from the lattice wave functions in an analysis; but with a degenerate ground state this is not possible, and a complicated Boltzmann distribution over coupled electron and lattice states must be treated. This is the major problem encountered in a treatment of the MCD in the present work. To resolve this problem, a formalism is used which reduces the calculation of a theoretical value for the zeroth moment of the MCD spectrum (or optical-absorption spectrum) to a calculation of the thermal expectation value of an operator; in the present case, this value can be computed by using Ham's treatment[20] of an orbital-triplet electronic state coupled to lattice modes of E_g symmetry.

The formalism used is essentially just an adaptation of some well-known results. The zeroth moments (integrals) of the spectra can be theoretically interpreted in terms of a dipole strength tensor $\vec{\vec{D}}$. For a transition between a single ground state $|g\rangle$ and a single excited state $|f\rangle$, the dipole strength tensor takes the form

$$\vec{\vec{D}} = \langle g|\vec{m}|f\rangle\langle f|\vec{m}|g\rangle, \tag{1}$$

where $\vec{m}$ is the electric dipole operator. Although the dipole strength is most convenient for present purposes, the connections with the moments of the spectra might be more transparent if made in terms of the familiar oscillator strength $\vec{\vec{f}}$[14,15]:

$$\vec{\vec{f}} = E\vec{\vec{D}}, \tag{2}$$

where E is simply the transition energy in rydbergs when the dipole strength is in atomic units.

The dipole strength (D_n) for light of a given polarization is a scalar that can be obtained by projecting the tensor onto the polarization vector.

$$D_n = \vec{e}_n^{\,*} \cdot \vec{\vec{D}} \cdot \vec{e}_n\,, \tag{3}$$

where $\vec{e}_n$ is a unit polarization vector which will be a complex vector if the light is elliptically or circularly polarized.

For cases with degenerate or nearly degenerate ground and/or excited states, the equation for the dipole strength can be conveniently generalized by considering $\langle g|$ as the complete ground-state manifold; that is, $\langle g|$ is a column of bras and $|g\rangle$ is a row of kets. The excited states can be considered similarly. With this convention, the need for summing and subscripting is reduced and a matrix representation for the dipole strength is obtained. A matrix representation can be convenient for computations since vector-coupling coefficients are often given in this form.

When the ground state is a nearly degenerate set of states, individual transitions are weighted according to their probability and a thermal average of the dipole strength is the quantity considered. This average, or expectation value, may be calculated using the thermodynamic density operator ρ, which is defined in terms of the system Hamiltonian H:

$$\rho = e^{-H/kT}/\mathrm{Tr}e^{-H/kT} . \quad (4)$$

The thermal expectation of the dipole strength is given by

$$\langle \vec{\vec{D}} \rangle = \langle g | \rho | g \rangle \langle g | \vec{m} | f \rangle \langle f | \vec{m} | g \rangle . \quad (5)$$

The notation can be made even more compact. Since the ground and excited states appear in the form of projection operators, it is possible to define

$$P_g = |g\rangle\langle g| , \quad P_f = |f\rangle\langle f| . \quad (6)$$

Furthermore, since the Hamiltonian and thermodynamics determine the ground state, it is completely defined by the density operator and for all cases of interest,

$$P_g \rho = \rho P_g \approx \rho I = \rho. \quad (7)$$

It is therefore possible to slightly modify the definition of $\vec{\vec{D}}$ and simply write

$$\vec{\vec{D}} = \vec{m} P_f \vec{m}, \quad (8)$$

$$\langle \vec{\vec{D}} \rangle = \mathrm{Tr}\,\rho \vec{\vec{D}} . \quad (9)$$

Dropping the ground-state functions in Eq. (8) is possible because they are restored by the density operator in Eq. (9). Equation (1) could be considered as giving a representation of $\vec{\vec{D}}$ as it is defined in Eq. (8).

Some possible advantages of this formulation may be seen. Since the thermal expection of the dipole strength is given in the form of a trace, it is basis invariant and it is also amenable to simple algebraic manipulation. Furthermore, the projection of the dipole strength onto a polarization basis now is considered as an operator, which is to be evaluated in the ground state, and properties such as its symmetry and commutation relations may be examined. In this respect, it may be noted that if P_f is a complete manifold of states it transforms as A_1 in the point group.

To interpret polarization-independent optical-absorption spectra, the dipole strength tensor is projected on to a random or arbitrary polarization basis ($\vec{e}_r$) and the projection will be simply denoted as D since it is a scalar operator associated with no specific polarization:

$$D = \vec{e}_r^{\,*} \cdot \vec{\vec{D}} \cdot \vec{e}_r = m_r P_f m_r . \quad (10)$$

For MCD spectra, it is convenient to define a rotatory strength operator R, which is simply the difference in the dipole strength of left- and right-circularly polarized light:

$$R = \vec{e}_- \cdot \vec{\vec{D}} \cdot \vec{e}_+ - \vec{e}_+ \cdot \vec{\vec{D}} \cdot \vec{e}_- = i(m_x P_f m_y - m_y P_f m_x), \quad (11)$$

where

$$\vec{e}_\pm = (\vec{e}_x \pm i\vec{e}_y)/\sqrt{2} \quad (12)$$

and subscripts + and − denote the left- and right-circular-polarization vectors for light propagating in the z direction.

The thermal expectation values of the D and R operators are, respectively, proportional to integrals of the experimentally determined optical absorption and MCD spectra:

$$\frac{1}{q}\int \frac{t\alpha(E)}{E}\,dE = \langle D \rangle = \mathrm{Tr}\,\rho D , \quad (13)$$

$$\frac{1}{q}\int \frac{t\Delta\alpha(E)}{E}\,dE = \langle R \rangle = \mathrm{Tr}\,\rho R . \quad (14)$$

Since there is a division by the photon energy E, which is only approximately a constant in the integrals, it is actually integrals or zeroth moments of optical shape functions that are considered.

The connection with the spectra requires little explanation; in spite of the terminology, the equations are only modified versions of the well-known[14,15] "Smakula equation." The major modification is just the division by E which accounts for the difference between the dipole strength considered here and the oscillator strength considered in the Smakula formula [see Eq. (2)]. The constant factor (q) will not be important here, but it is essentially the same factor which appears in the Smakula formula. It is approximately given by

$$q = (4\pi^2 Nt/nc\hbar)[\tfrac{1}{3}(n^2+2)]^2 , \quad (15)$$

where N is the number of impurity ions per unit volume, n is the refractive index, and t is the sample thickness.

Equations (13) and (14) give a means of comparing experimental results and predictions of a theo-

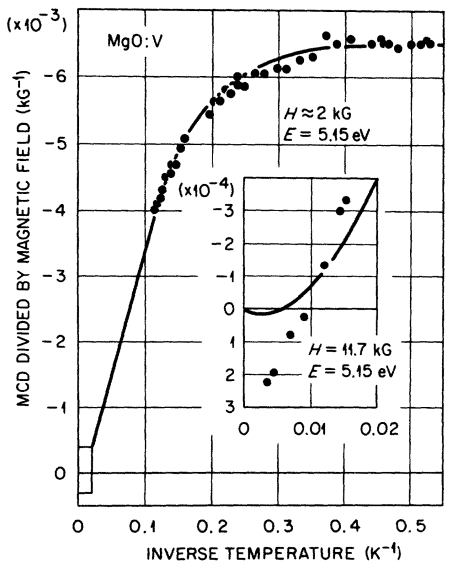

FIG. 4. Temperature dependence of the MCD at 5.15 eV, and a parametric fit to the data.

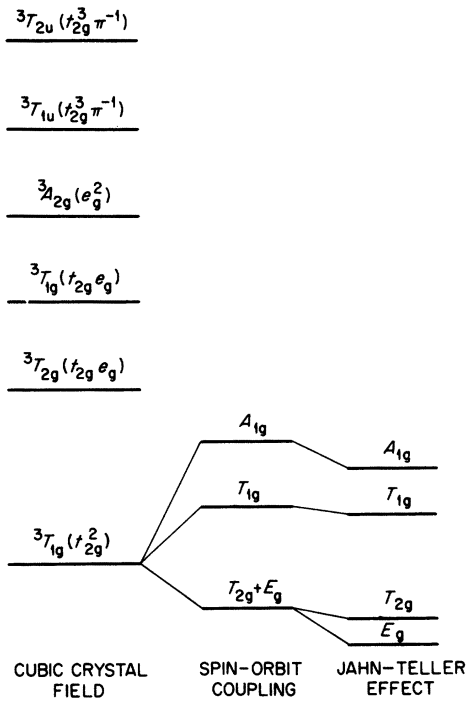

FIG. 5. Energy-level diagram for the V^{3+} ion in MgO. The Jahn-Teller interaction is actually assumed the largest perturbation, but it changes the qualitative diagram only in second order.

retical model. In principle, the model can be defined by a Hamiltonian, which can be used to generate the projector P_f and to define density operator ρ; and the calculation can be performed in an arbitrary basis. However, in order to make the present calculations tractable, a simpler approach is adopted and some approximations are made. First, the symmetry of the manifold of excited-state electron orbitals which give a representation of P_f will be assumed. Actually, two possibilities are considered and the final choice is based upon agreement with the experimental results. The lattice and spin states will not be explicitly included in P_f, since closure over the lattice and spin space will be assumed and they will give only identity operators in the projector. Second, the trace will be evaluated in a basis which approximately diagonalizes the Hamiltonian so that only a ground-state Hamiltonian is required to define the density operator. In other words, the $^3T_{1g}$ ground state which diagonalizes the free-ion plus crystal-field Hamiltonian is assumed and only a reduced Hamiltonian for this manifold is considered further. Third, the problem of treating coupled electronic and lattice wave functions in the ground state, where closure of the lattice states cannot be invoked, will be met by using the approximations given by Ham for an orbital-triplet electronic state coupled to lattice modes of E_g symmetry. Justifiably or not, any coupling to T_{2g} lattice modes is neglected. The adoption of Ham's results greatly facilitates the calculations; it supplies a parametric description of the electron-lattice interaction; it defines the effect of this interaction on the dipole and rotatory strength operators; it gives the required ground-state Hamiltonian; it makes explicit reference to the lattice states unnecessary. Fourth, the Zeeman interaction will be considered only in the ground state and only as a first-order perturbation. Any MCD due to magnetically induced mixing of the ground or excited states with other manifolds is therefore neglected. Fifth, second-order perturbations which originate because of the electron-lattice interaction will be included in the density operator, but will not be included in the Zeeman interaction or in the evaluation of the rotatory strength operator.

An energy-level diagram for the V^{3+} ion in MgO is shown in Fig. 5. The symmetry and ordering of the Stark-split V^{3+} states and two low-energy charge-transfer states are indicated on the left. The occupied one-electron orbitals corresponding to each state are indicated according to their strong crystal-field classification. (Coulomb interactions admix these strong field orbitals.) π^{-1} is used to denote a hole in a ligand π orbital. The symmetry classification and ordering of the ion states is well known[2,21] and need not be considered here. On the other hand, the charge-transfer states are more difficult to classify. These states result from the transfer of an electron from a high-energy ligand orbital to the lowest-energy vanadium orbital. Usually, the π orbitals are placed at higher energy than the σ orbitals and the πt_{2u} orbital is placed above the πt_{1u} orbital.[2,12,13] The $^3T_{1u}(t_{2g}^3\pi^{-1})$ and $^3T_{2u}(t_{2g}^3\pi^{-1})$ states result from coupling the occupied ion orbitals with a πt_{2u} or πt_{1u} ligand hole, respectively. One of these is assumed to be the excited state of the transition, and the choice of symmetry for the states giving a representation of P_f is based upon this assumption.

The splitting of the $^3T_{1g}$ ground-state manifold is also indicated in Fig. 5 and is described in more detail in Refs. 5 and 7. A Jahn-Teller effect alone does not remove the degeneracy of the $^3T_{1g}$ ground state. It does associate a different lattice distortion with each electronic orbital of the Cartesian basis which diagonalizes the electron-lattice interaction. Even when a spin-orbit interaction (which is here assumed smaller than the electron-lattice interaction) is added to first order, the energy-level diagram is qualitatively the same as in the absence of a Jahn-Teller effect.[20,22] Spin-orbit splittings are reduced by a Jahn-Teller effect, but only in second order is the energy-level diagram qualitatively changed. A spin-orbit in-

teraction between the ground and higher lying vibronic levels does split the lowest spin-orbit multiplet into a triplet and a doublet with the latter lowest; the ordering of energy levels indicated on the right-hand side of Fig. 5 results.

The effective Hamiltonian which summarizes the ground-state splittings has been given by Ham[20] and is assumed here:

$$H_0 = \gamma g_L \lambda \vec{L}\cdot\vec{S} + K_1(\vec{L}\cdot\vec{S})^2 + K_2(L_x^2S_x^2 + L_y^2S_y^2 + L_z^2S_z^2), \quad (16)$$

where

$$K_1 = -(\lambda^2 g_L^2/\hbar\omega)e^{-x}G(\tfrac{1}{2}x)\,, \quad (17)$$

$$K_2 = -(\lambda^2 g_L^2/\hbar\omega)e^{-x}[G(x) - G(\tfrac{1}{2}x)]\,; \quad (18)$$

$$\gamma \equiv e^{-x/2}, \quad x \equiv \frac{3E_{JT}}{\hbar\omega}, \quad G(x) \equiv \sum_{n=1}^{\infty}\frac{x^n}{n(n!)}\,.$$

E_{JT} is the Jahn-Teller energy and $\hbar\omega$ is the vibrational quantum. The factor γ actually is a lattice-function overlap integral which arises because the different electronic orbitals are associated with different lattice displacements. It reduces electronic operators that are off diagonal with respect to electronic orbitals in a Cartesian basis. The function $G(x)$ originates in summing second-order effects over higher vibronic levels.

The magnetic field perturbation H_z must be added to H_0. Again by following Ham's work,[20] we find

$$H_z = -\vec{\mu}\cdot\vec{H} = \mu_B H(\gamma g_L L_z + 2S_z)\,. \quad (19)$$

H_z will be considered a small perturbation and will be considered in the limit $\mu_B H \ll kT$.

A computation of the ground-state-energy values is readily performed using Griffith's tables of vector-coupling coefficients.[21] Using Griffith's complex basis functions and notation, we find

$$E_g\theta: -\gamma'\lambda + K_1 + 2K_2,$$

$$E_g\epsilon: -\gamma'\lambda + K_1 + 2K_2,$$

$$T_{2g}0: -\gamma'\lambda + K_1 + K_2\,,$$

$$T_{2g}\pm 1: -\gamma'\lambda + K_1 + K_2 \mp \tfrac{1}{2}(2-\gamma')\mu_B H,$$

$$T_{1g}0: \gamma'\lambda + K_1 + K_2,$$

$$T_{1g}\pm 1: \gamma'\lambda + K_1 + K_2 \pm \tfrac{1}{2}(2-\gamma')\mu_B H,$$

$$A_{1g}a_1: 2\gamma'\lambda + 4K_1 + 2K_2,$$

where $\gamma' \equiv -g_L\gamma$. In first order, the magnetic field lifts the degeneracy of the triplets but not the degeneracy of the doublet.

The effect of the electron-lattice interaction on the Hamiltonian and, therefore, the density operator is described in Eqs. (16)–(19). The further effect of the electron-lattice interaction on R may be inferred by noting that it is an off-diagonal operator that transforms as L_z [see Eq. (11)]. First-order effects are therefore included by simply making the substitution $R \to \gamma R$.[20] This substitution completes a parametric description of the electron-lattice interaction that enables a calculation of $\langle R\rangle$ using only electron wave functions.

Using only symmetry, $\langle R\rangle$ can be calculated to within reduced matrix elements of the electric dipole operator. One method is to evaluate the various operators using the ground-state functions ($|g\rangle$) which diagonalize $H_0 + H_z$ to first order in the magnetic field. Perturbation theory defines these functions in terms of the octahedral basis functions ($|\Gamma M_\Gamma\rangle$) which diagonalize H_0:

$$|g\rangle = |\Gamma M_\Gamma\rangle + |\Gamma' M_{\Gamma'}\rangle\frac{\langle\Gamma' M_{\Gamma'}|H_z|\Gamma M_\Gamma\rangle}{E_\Gamma - E_{\Gamma'}}\,. \quad (20)$$

A matrix representation for $\langle R\rangle$ can then be obtained in the form

$$\langle R\rangle = \gamma H\,\mathrm{Tr}\,\langle\Gamma M_\Gamma|(e^{-H_0/kT}/Z_0)|\Gamma M_\Gamma\rangle \times[\langle\Gamma M_\Gamma|(\mu/kT)|\Gamma M_\Gamma\rangle + 2\langle\Gamma M_\Gamma|\mu|\Gamma' M_{\Gamma'}\rangle/(E_{\Gamma'} - E_\Gamma)]\langle\Gamma M_\Gamma|R|\Gamma M_\Gamma\rangle\,, \quad (21)$$

where

$$Z_0 \equiv \mathrm{Tr}\,\langle\Gamma M_\Gamma|e^{-H_0/kT}|\Gamma M_\Gamma\rangle\,.$$

The first factor in the square brackets contains the diagonal matrix elements of μ and the second factor contains the off-diagonal elements. The matrix elements of μ and R can be evaluated in the $|M_s M_L\rangle$ basis where they are diagonal and can be converted to the $|\Gamma M_\Gamma\rangle$ basis, where H_0 is diagonal using Griffith's coupling coefficients.

Another method of making the calculation is to utilize operator concepts and replace R by its operator equivalent L_z. The expectation value of L_z may be calculated from the partition function Z:

$$Z = \mathrm{Tr}\rho\,, \quad (22)$$

$$\langle R\rangle \sim \langle L_z\rangle = \frac{kT}{\mu_B}\frac{\partial \ln Z}{\partial(\gamma' H)}\,. \quad (23)$$

This method gives $\langle R\rangle$ to within a constant that is easily determined in the high-temperature limit where the density operator may be expanded in powers of inverse temperature. In any case, the result to first order in magnetic field is

$$\langle R\rangle = \pm\mu_B H\gamma\,|m|^2\left[-\frac{2+\gamma'}{3(2\gamma'\lambda - K_2)} - \frac{2-\gamma'}{K_2} + \left(-\frac{2+\gamma'}{4\gamma'\lambda} + \frac{2-\gamma'}{K_2} + \frac{2-\gamma'}{4kT}\right)e^{+K_2/kT}\right.$$

$$+\left(\frac{2+\gamma'}{4\gamma'\lambda}+\frac{2+\gamma'}{3(2\gamma'\lambda-K_2)}-\frac{2(2+\gamma')}{3(\gamma'\lambda+3K_1+K_2)}+\frac{2-\gamma'}{4kT}\right)e^{-(2\gamma'\lambda-K_2)/kT}$$

$$+\frac{2(2+\gamma')}{3(\gamma'\lambda+3K_1+K_2)}e^{-(3\gamma'\lambda+3K_1)/kT}\Big](2+3e^{+K_2/kT}+3e^{-(2\gamma'\lambda-K_2)/kT}+e^{-(3\gamma'\lambda+3K_1)/kT})^{-1}, \quad (24)$$

where m denotes a reduced matrix element of the electric dipole operator, and the + or − sign is for T_{1u} or T_{2u} excited-state symmetry, respectively. An excited-state-symmetry assignment can be based upon this sign difference.

Similar calculations give $\langle D\rangle$, which is calculated without the magnetic field perturbation. D is a diagonal operator and is therefore not reduced by the electron-lattice interaction. It transforms as A_1, its expectation value is temperature independent, and it can be evaluated in the limit of infinite temperature:

$$\langle D\rangle = \tfrac{1}{3}|m|^2. \quad (25)$$

V. ANALYSIS

Although the expression for $\langle R\rangle$ is quite complicated, most of the parameters are not independently adjustable. The spin-orbit parameter may be estimated from the free-ion value[21] ($\lambda \approx 105\,\mathrm{cm}^{-1}$) and the orbital g value may be estimated using crystal-field theory for the d-shell splitting of the ion ($g_L \approx -1.25$).[2,5] The reduced matrix element of the electric dipole operator m appears in both $\langle D\rangle$ and $\langle R\rangle$ so that ratios independent of this parameter can be evaluated. The only other parameters entering the expression are the Jahn-Teller energy E_{JT} and the vibrational quantum $\hbar\omega$. The vibrational quantum has been estimated from experiments on phonon sidebands in MgO ($\hbar\omega \approx 450\ \mathrm{cm}^{-1}$).[5,7,23] Hence, rough values may be assumed for all significant parameters except E_{JT}.

Equation (24) could be directly fit to the temperature-dependent MCD data, with E_{JT} as an adjustable parameter. However, the data are discontinuous and have already been reasonably well fit to a model assuming a tetragonal site symmetry.[2] Hence, such exact treatment may not be justified; it is, however, unnecessary for establishing the compatibility of the data with the present model. Since the data cover two orders of magnitude in temperature, the expression for $\langle R\rangle$ can be approximated in various temperature ranges: for $kT > 3\gamma'\lambda$,

$$\langle R\rangle \rightarrow \mp\tfrac{1}{3}\mu_B H\gamma\,|m|^2(\gamma'/kT); \quad (26)$$

for $2\gamma'\lambda > kT > -K_2$,

$$\langle R\rangle \rightarrow \pm\mu_B H\gamma\,|m|^2\left(\frac{2-\gamma'}{4kT}-\frac{2+\gamma'}{12\gamma'\lambda}\right) \equiv \left(B+\frac{C}{kT}\right)H; \quad (27)$$

for $-K_2 > kT$,

$$\langle R\rangle \rightarrow \pm\tfrac{1}{2}\mu_B H\gamma\,|m|^2\left(-\frac{2-\gamma'}{K_2}-\frac{2+\gamma'}{3(2\gamma'\lambda-K_2)}\right) \equiv SH. \quad (28)$$

The parameters B and C, defined in Eq. (27), are proportional to the Faraday parameters,[18] often used to describe MCD when a linear expansion in terms of H and H/T is valid. The parameter S of Eq. (28) has been added to describe the saturation value of the MCD. It is also convenient to use the parameter $D \equiv \langle D\rangle$, if context precludes confusion with the operator.

The three approximate relations are adequate for an examination and interpretation of the experimental data. They can be used to determine the following: (i) the qualitative correspondence of the model and the data; (ii) the choice between T_{1u} and T_{2u} excited-state symmetry; (iii) whether a dynamic Jahn-Teller interaction is indicated by the data; (iv) approximate values for the electron-lattice interaction parameters describing the Jahn-Teller effect.

An examination of the approximate relations shows that the MCD, which is proportional to $\langle R\rangle$, should be small at high temperatures and increase in magnitude with decreasing temperature to a maximum, then decrease through zero, and increase in magnitude until saturating at a constant value at yet lower temperature. (The reader is reminded that the saturation is at low magnetic field.) The data do show this behavior except for the initial increase to a maximum, which presumably occurs at still higher temperature than that of the measurements; or possibly it is masked by small contributions due to magnetically induced mixing of either the ground or excited states with other states that are not considered here. The sign of the MCD is consistent with an excited-state-symmetry classification as $^3T_{2u}$. This implies that, contrary to the usual ordering of the ligand-orbital energy levels, the πt_{1u} state is above the πt_{2u} state. The saturation at low temperature and low magnetic field implies a zero-field splitting of the ground state, with a nonmagnetic level lowest. This is consistent with the predictions of the Jahn-Teller model.

In order to determine values for the various parameters, the experimental values B, C, D, and S have been defined and related to the predictions of the model. Using ratios of $\langle R\rangle$ to $\langle D\rangle$ the fol-

lowing approximate connection between the parameters and the experimental data is made:

$$B/D = \gamma(2+\gamma')\mu_B/4\gamma'\lambda = 4.25\times10^{-3}\ \mu_B/\mathrm{cm}^{-1}\ , \tag{29}$$

$$C/D = -\tfrac{3}{4}\gamma(2-\gamma')\mu_B = -2.62\times10^{-1}\mu_B\ , \tag{30}$$

$$S/D = \tfrac{3}{2}\gamma\left(\frac{2-\gamma'}{K_2}+\frac{2+\gamma'}{3(2\gamma'\lambda-K_2)}\right)\mu_B = -5.25\times10^{-2}\ \mu_B/\mathrm{cm}^{-1}\ . \tag{31}$$

Since the temperature-dependent data are for the MCD peak value, the experimental numbers are calculated using the ratio of integrated MCD to the peak value. There is a large uncertainty in assuming a background base line for the optical-absorption spectrum and in extrapolating the temperature-dependent MCD data. As a result, the numerical values are easily uncertain by 20%.

Assuming the estimates of $g_L = -1.25$ and $\lambda = 105\ \mathrm{cm}^{-1}$, the parameters of the Jahn-Teller model can be calculated in several ways. Values for $\gamma \approx 0.2$ are obtained from the ratios B/D, C/D, and C/B. Using this γ value and the ratios S/D and S/C, an estimate for $K_2 \approx -9.4\ \mathrm{cm}^{-1}$ is obtained. The γ value implies a Jahn-Teller energy that is roughly equal to the vibrational quantum ($E_{JT} \approx \hbar\omega$) estimated as 400–500 cm^{-1}. As a check on the estimate of the vibrational quantum and the consistency of the results, the parameters can be used in Eq. (18) and $\hbar\omega$ is calculated to be approximately 500 cm^{-1}.

The fit to the data obtained using the parameters is indicated on Fig. 4. The agreement appears to be satisfactory. The discrepancy at high temperatures (shown in the insert) has little statistical significance, but it is possibly of interest. The small difference can easily be attributed to a magnetically induced mixing of levels that has not been considered. On the other hand, the slope of the curve where it intercepts the origin is a sensitive function of γ and the point where the curve crosses the axis depends on the spin-orbit parameter λ [see Eqs. (26) and (27)]. Hence, a larger γ and a smaller λ would give better agreement with the high-temperature results. A reduction of λ could be attributed to covalency, but a larger γ would not fit the low-temperature data as well. It can be expected that γ increases at temperatures where higher vibronic levels are occupied; however, with $\hbar\omega \approx 450\ \mathrm{cm}^{-1}$ any such increase, here, is probably small.

VI. DISCUSSION AND CONCLUSION

It has been shown that the MCD data quite reasonably fit a Jahn-Teller active ground state where second-order effects split the ground state so that a nonmagnetic doublet is lowest. Values for the various Jahn-Teller parameters are found to be reasonably consistent among themselves. However, they differ somewhat from values deduced from APR measurements. Ray's analysis implies $\gamma \approx 0.4$; the analysis of Buisson and Nahmani implies $\gamma \approx 0.6$; Bates *et al.* give $\gamma \approx 0.15$ based upon a different ground-state splitting. The MCD data, as analyzed here, give $\gamma \approx 0.2$. Estimates of the Jahn-Teller energy E_{JT} are correspondingly different also. The neglect of second-order effects in the rotatory strength and the Zeeman perturbation may be partially responsible for the discrepancy. Experimental errors (e.g., depolarization effects), if any, would most probably reduce the MCD and could also lead to an underestimate of γ. The ground-state splitting ($-K_2 = 9.4\ \mathrm{cm}^{-1}$) is in good agreement with the previous estimates by Brabin-Smith and Rampton (10.2 cm^{-1}) using APR[1] and by Modine (10 cm^{-1}) using MCD,[2] even though these previous estimates were based upon an assumed tetragonal site symmetry. It also compares reasonably well with the 7-cm^{-1} splitting found by Buisson and Nahmani.

The value of $g \approx 0.87$ calculated for the T_{2g} state from the MCD (using $g \approx 1 + \frac{1}{2}\gamma g_L$) is higher than the $g \approx 0.68$ determined from the more accurate APR measurements. However, as shown by Ray,[5] there is a second-order correction to the g value. This correction which was neglected in the MCD analysis would reduce the discrepancy. Also, it is difficult to relate the g value from the APR measurements to the g value determined from the MCD. The APR shows a very broad asymmetric resonant absorption, presumably due to strain broadening, and $g = 0.69$ is considerably less than the average g for this absorption. Only an average g can be determined from the MCD, and the effect of strain on the MCD has not been considered.

Although the interpretation of the ground-state splitting in terms of a second-order effect now appears correct, it was previously shown[2] that the MCD data reasonably fit a model based upon a tetragonal site symmetry, and a tetragonal symmetry has also been proposed in explanations of the Brabin-Smith–Rampton APR results.[1,3] Although a different ordering of the ground-state levels was proposed in each case, only one such ordering could be correct. This ordering requires a singlet state A_1 lowest. Brabin-Smith and Rampton also placed a singlet lowest but assigned it a B_2 symmetry. Other investigators have postulated or considered a doublet (B_1+B_2) lowest, and assumed that it is nonmagnetic.[3,5] However, this doublet in D_{4h} symmetry can be split by a magnetic field. If a magnetic doublet were lowest, the MCD would not saturate at low magnetic fields. Hence, such an assignment is forbidden by the MCD results.

The MCD implies a symmetry assignment for the excited state of the transition. The symmetry assignment of $^3T_{2u}$ for this charge-transfer state and the implied placement of the πt_{1u} ligand orbital at higher energy than the πt_{2u} would be surprising except that the ordering of these orbitals has also been reversed by similar MCD studies of some of the 5*d* hexahalides.[24] There is the possibility that this reversal in the order of the ligand levels may be general. It is hoped that such MCD symmetry classifications will stimulate a theoretical consideration of these ligand orbitals.

It appears that MCD originating from a Jahn-Teller active ground state can be analyzed with reasonable success. The analysis presented is more complicated than that required for orbitally nondegenerate ground states, but it is hardly prohibitive. It might be possible to add second-order terms to the rotatory strength and the Zeeman interaction and to more precisely treat the data. However, the analysis presented appears to encompass the essentials of the problem.

ACKNOWLEDGMENTS

The experimental data presented here originated as a part of a doctoral dissertation presented to the Department of Physics and the Graduate School of the University of Oregon. The important contributions to this work that were made possible by that institution are gratefully acknowledged. Professor J. C. Kemp is thanked for initiating the author's interest in magneto-optics and for his sponsorship of the dissertation.

†Research sponsored jointly by ARPA through the Air Force Office of Scientific Research under contract with the University of Oregon (Contract No. 70-1912) and the U.S. Atomic Energy Commission under contract with the Union Carbide Corporation.

[1]R. G. Brabin-Smith and V. W. Rampton, J. Phys. C 2, 1759 (1969).
[2]F. A. Modine, thesis (University of Oregon, 1971) (unpublished).
[3]C. A. Bates, L. C. Goodfellow, and K. W. H. Stevens, J. Phys. C 3, 1831 (1970).
[4]T. Ray, Solid State Commun. 9, 911 (1971).
[5]T. Ray, Phys. Rev. B 5, 1758 (1972).
[6]R. Buisson and A. Nahmani, Phys. Lett. 37, 9 (1971).
[7]R. Buisson and A. Nahmani, Phys. Rev. B 6, 2648 (1972).
[8]S. N. Jasperson and S. E. Schnatterly, Rev. Sci. Instrum. 40, 761 (1969).
[9]D. D. Kasarda, J. E. Bernardin, and W. Gaffield, Biochem. 7, 3950 (1968).
[10]M. D. Sturge, Phys. Rev. 130, 639 (1962).
[11]R. W. Soshea, A. J. Dekker, and J. P. Sturtz, J. Phys. Chem. Solids 5, 23 (1958).
[12]H. H. Tippins, Phys. Rev. B 1, 126 (1970).
[13]D. S. McClure, Solid State Phys. 9, 400 (1959).
[14]D. L. Dexter, Solid State Phys. 6, 353 (1958).
[15]W. B. Fowler, *Physics of Color Centers*, edited by W. B. Fowler (Academic, New York, 1968).
[16]C. H. Henry, S. E. Schnatterly, and C. P. Slichter, Phys. Rev. 137, A583 (1965).
[17]C. H. Henry and C. P. Slichter, *Physics of Color Centers*, edited by W. B. Fowler (Academic, New York, 1968).
[18]A. D. Buckingham and P. J. Stephens, Ann. Rev. Phys. Chem. 17, 399 (1966).
[19]P. J. Stephens, J. Chem. Phys. 52, 3489 (1970).
[20]F. S. Ham, Phys. Rev. 138, A1727 (1965).
[21]J. S. Griffith, *The Theory of Transition Metal Ions* (Cambridge U. P., Cambridge, England, 1961).
[22]M. D. Sturge, Solid State Phys. 20, 91 (1967).
[23]M. J. L. Sangster and C. W. McCombie, J. Phys. C 3, 1498 (1970).
[24]S. B. Piepho, J. R. Dickinson, J. A. Spencer, and P. N. Schatz, J. Chem. Phys. 57, 982 (1972), and references therein.

PHYSICAL REVIEW B VOLUME 8, NUMBER 2 15 JULY 1973

Optical Properties of Mn^{2+} in Pure and Faulted Cubic ZnS Single Crystals

B. Lambert, T. Buch, and A. Geoffroy
Laboratoire de Luminescence II, Université de Paris VI-75005, Paris, France*
(Received 16 October 1972)

It is shown that a number of lines in the excitation and emission spectra of Mn^{++} in ZnS single crystals are associated with the presence of stacking faults in predominantly cubic crystals. The position of these lines is interpreted in terms of the modification of the cubic crystal field at the faulted sites.

I. INTRODUCTION

The optical properties of Mn^{++} and other impurities in ZnS host crystals have been studied rather extensively, especially due to the great interest in variously doped ZnS as synthetic phosphors, where Mn^{++} plays the role of an efficient activator.[1] The essential aspects of the absorption and emission